Molecular Therapy
Original Article

Neutrophils Deficient in Innate Suppressor IRAK-M Enhances Anti-tumor Immune Responses

Yao Zhang,[1,4] Na Diao,[1,2,4] Christina K. Lee,[1] Hong Wei Chu,[3] Lan Bai,[2] and Liwu Li[1]

[1]Department of Biological Sciences, Virginia Tech, Blacksburg, VA 24061, USA; [2]Guangdong Provincial Key Laboratory of Gastroenterology, Department of Gastroenterology, Nanfang Hospital, Southern Medical University, Guangzhou, Guangdong 510515, PR China; [3]Department of Medicine, National Jewish Health, Denver, CO 80206, USA

Tumor-associated immune-suppressive neutrophils are prevalent in various cancers, including colorectal cancer. However, mechanisms of immune-suppressive neutrophils are not well understood. We report that a key innate suppressor, IRAK-M (interleukin-1 receptor-associated kinase M), is critically involved in the establishment of immune-suppressive neutrophils. In contrast to the wild-type (WT) neutrophils exhibiting immune-suppressive signatures of CD11b^{high}PD-L1^{high} CD80^{low}, IRAK-M-deficient neutrophils are rewired with reduced levels of inhibitory molecules PD-L1 and CD11b, as well as enhanced expression of stimulatory molecules CD80 and CD40. The reprogramming of IRAK-M-deficient neutrophils is mediated by reduced activation of STAT1/3 and enhanced activation of STAT5. As a consequence, IRAK-M-deficient neutrophils demonstrate enhanced capability to promote, instead of suppress, the proliferation and activation of effector T cells both *in vitro* and *in vivo*. Functionally, we observed that the transfusion of IRAK-M$^{-/-}$ neutrophils can potently render an enhanced anti-tumor immune response in the murine inflammation-induced colorectal cancer model. Collectively, our study defines IRAK-M as an innate suppressor for neutrophil function and reveals IRAK-M as a promising target for rewiring neutrophils in anti-cancer immunotherapy.

INTRODUCTION

Colorectal cancer (CRC) is among the top three most common cancers affecting both men and women in the United States, with >140,000 cases diagnosed annually, and still remains as one of the leading causes of cancer-related morbidity worldwide.[1] Recent studies reveal the presence of diverse innate and adaptive immune cells within CRC tissues.[2] Current immunotherapeutic approaches primarily focusing on the adaptive immune system through tumor vaccines, engineered T cells, and checkpoint inhibition only demonstrate limited success.[2,3] These studies suggest that targeting adaptive immune cells alone may not be sufficient to render effective anti-cancer therapy and demonstrate the critical need to better characterize the less-explored innate immune cells. With particular relevance, innate neutrophils are the most abundant immune cells, constituting >50% of all leukocytes. The numbers of circulating neutrophils are further increased in patients with cancers including CRC, especially in patients with advanced-stage cancer.[4,5] Translational studies through the last decade reveal that a higher ratio of tumor-associated neutrophils is a robust predictor of poor clinical outcomes in many solid tumors, including CRC.[5,6] Recent studies reveal that neutrophils may support tumor growth through inhibiting CD8 T cells and inducing CD8 T cell apoptosis,[7–9] and such inhibition can be released through applying a transforming growth factor β (TGF-β) inhibitor.[10] Tumor-associated neutrophils may compromise the anti-cancer immune response through expressing co-inhibitory molecules such as programmed death ligand 1 (PD-L1) and suppressing T cell proliferation and activation.[11,12] Clinical studies further reveal that cancer patients may have heterogeneous neutrophil populations with both immune-enhancing (N1) and immune-inhibiting (N2) phenotypes.[13,14] Consequently, attempts to deplete immune-suppressive neutrophils have been shown to have beneficial effects in reducing tumor progression.[15,16] Together, these studies point to an intriguing potential of re-programming neutrophils in cancer treatment. Despite its compelling prognostic value, the mechanisms underlying the tumor-promoting or inhibiting activity of neutrophils are poorly understood.

Neutrophils are not only known to be closely associated with tumorigenesis but may also be utilized to treat cancer if properly reprogrammed.[15–17] Neutrophil-based therapies hold significant advantages over traditional cancer therapies or emerging T cell-based immune therapy; neutrophil is the first natural responder to any abnormal situations including inflammation and cancer growth[18,19] and has the innate ability to home into tumor tissues. Therefore, neutrophil-based therapies eliminate key caveats, including challenges in effective

Received 13 July 2019; accepted 12 September 2019;
https://doi.org/10.1016/j.ymthe.2019.09.019.

[4]These authors contributed equally to this work.

Correspondence: Liwu Li, Department of Biological Sciences, Virginia Tech, 970 Washington Street, Blacksburg, VA 24061-0910, USA.
E-mail: lwli@vt.edu
Correspondence: Lan Bai, Guangdong Provincial Key Laboratory of Gastroenterology, Department of Gastroenterology, Nanfang Hospital, Southern Medical University, 1838 Guangzhou North Avenue, Guangzhou, Guangdong 510515, PR China.
E-mail: bailan16399@163.com
Correspondence: Yao Zhang, Department of Biological Sciences, Virginia Tech, 970 Washington Street, Blacksburg, VA 24061, USA.
E-mail: zhang152@vt.edu

targeting to tumor tissues facing traditional bio-based therapies. Recent progress has demonstrated that neutrophils can be used as an effective vehicle to deliver anti-cancer drugs to solid tumors.[18] Second, neutrophils homed into cancer tissues may readily communicate with ever-evolving immune cells (e.g., T cells, natural killer [NK] cells, etc.) present in the tumor tissues.[7] If properly programmed, tumor-homing neutrophils may naturally expand/activate existing tumor-associated immune-cells within the changing tumor immune environment, avoiding the limitation associated with chimeric antigen receptor (CAR)-T therapies, which require constant engineering of T cells targeting evolving tumor antigens.[20] In order to better harness the significant potential of neutrophils in anti-cancer therapy, however, we must have a clear understanding of neutrophil reprogramming dynamics responsible for the immune-inhibiting versus immune-enhancing effects on the tumor immune environments.

The interleukin-1 receptor-associated kinase M (IRAK-M) is one of the signaling suppressors in innate leukocytes, such as monocytes and macrophages.[21,22] IRAK-M levels are significantly elevated in human patients with colitis-associated neoplasia as well as advanced stages of CRC.[23] IRAK-M$^{-/-}$ mice are resistant to inflammation-driven tumorigenesis in the colon.[23,24] However, the role of IRAK-M in regulating neutrophil activation in the context of CRC is not well understood.

In this study, we examined the mechanisms responsible for the generation of immune-suppressive neutrophils mediated by IRAK-M *in vitro* and *in vivo*. Comparing wild-type and IRAK-M$^{-/-}$ neutrophils, our study revealed that IRAK-M not only facilitates the expression of immune-suppressive mediator PD-L1, but also suppresses the expression of immune-enhancing mediators CD80 and CD40 in neutrophils. Collectively, we found that enhanced CD80/CD40 expression and reduced expression of PD-L1 on IRAK-M$^{-/-}$ neutrophils led to the re-wiring of neutrophils into an immune-enhanced state for an effective anti-tumor defense. Extending previous findings that IRAK-M-deficient mice are protected from inflammation-induced colon cancer, we further found that IRAK-M$^{-/-}$ neutrophils can sufficiently render an enhanced anti-tumor response in an inflammation-mediated CRC model.

RESULTS

IRAK-M Supports AOM/DSS-Induced CRC Progression

Our previous study reported that IRAK-M is significantly upregulated in human patients with colitis-associated neoplasia as well as advanced stages of CRC.[23] Furthermore, we found that IRAK-M$^{-/-}$ mice were significantly protected against dextran sulfate sodium (DSS)-mediated gastrointestinal (GI) inflammation and azoxymethane (AOM)/DSS-mediated tumor formation.[23] In this current study, we first confirmed our previous report that IRAK-M$^{-/-}$ mice were significantly protected against DSS-mediated GI inflammation and AOM/DSS-mediated tumor formation. Compared to wild-type (WT) mice, the IRAK-M$^{-/-}$ mice showed both decreased tumor numbers and reduced tumor size (Figure 1A). In particular, the average numbers of microscopic (<2-mm diameter) and macroscopic (≥2-mm diameter) polyps in WT mice (12.5 ± 1.3, 6.0 ± 0.7, respectively) were about 3–4 times higher than that in IRAK-M$^{-/-}$ mice (3.9 ± 0.6, 1.5 ± 0.7) (Figure 1C). Moreover, IRAK-M$^{-/-}$ mice displayed reduced weight loss (Figure 1D) and much lower disease scores (Figure 1E) during the course of AOM/DSS treatment, suggesting an attenuation of disease progression compared to the WT counterparts. Histologically, compared to IRAK-M$^{-/-}$ mice, WT mice presented widespread inflammation throughout the mucosa with alterations of epithelia structure, loss of crypts, and enhanced inflammatory cell infiltration (Figure 1F). Likewise, Ki67 immunostaining of colon tissue showed that IRAK-M$^{-/-}$ mice displayed a significant reduction in proliferating cell number as compared with WT ones (Figure 1G). Collectively, our data reveals that IRAK-M-deficient mice exhibit dramatic resistance to tumorigenesis when challenged with AOM/DSS.

IRAK-M Deficiency in Neutrophils Enhances Immune-Activating Signals and Inhibits Immune Checkpoint Signals

Since IRAK-M is a well-known innate immune suppressor, we tested whether enhanced anti-tumor defense in IRAK-M$^{-/-}$ mice may be due to more effective anti-cancer checkpoints from innate immune cells such as neutrophils. Therefore, we tested neutrophil distribution (defined as the percentage of CD11b^{+}Ly6G^{+} cells out of total number of cells), several key innate checkpoint molecules, including PD-L1/CD11b as well as activating molecules such as CD80/CD40 on neutrophils. As shown in Figures 2A and 2B, the percentages of neutrophils within spleen and blood were significantly higher in naive IRAK-M$^{-/-}$ mice than that in naive WT mice. After the challenge of AOM/DSS, the percentages of neutrophils in spleen and colon were significantly increased in WT mice as compared to IRAK-M$^{-/-}$ mice (Figure 2A; Figure S1). Meanwhile, the percentages of neutrophils within blood remained similar between WT and IRAK-M$^{-/-}$ mice after the AOM/DSS challenge (Figure 2B). Intriguingly, we observed that neutrophils in spleen from naive IRAK-M$^{-/-}$ mice expressed significantly lower PD-L1 and CD11b than WT mice (Figure 2C). After AOM/DSS treatment, neutrophils in spleen from IRAK-M$^{-/-}$ mice not only expressed significantly lower PD-L1, CD11b, and LRRC32 but also higher CD80 and CD40 (Figure 2D). Similarly, IRAK-M$^{-/-}$ neutrophils in blood expressed lower PD-L1, CD11b, and higher CD80 before or after AOM/DSS treatment, as well as higher CD40 after AOM/DSS treatment (Figures 2E and 2F). IRAK-M$^{-/-}$ neutrophils in colon also expressed higher CD40 and CD80 after AOM/DSS challenge (Figure S1). In summary, our data demonstrate that IRAK-M deficiency rewires neutrophils from the CD11b^{high}PD-L1^{high}CD80^{low} CD40^{low} immune-suppressive phenotype to the CD11b^{low}PD-L1^{low}CD80^{high}CD40^{high} immune-enhancing phenotype, revealing a key role of IRAK-M in the generation of immune-suppressive neutrophils during progression of AOM/DSS-induced colorectal tumor.

Enhanced T Cell Activation in IRAK-M$^{-/-}$ Mice Challenged with AOM/DSS

Neutrophils have been well associated with immunosuppression of adaptive immunity.[25] As we documented above, we speculated that

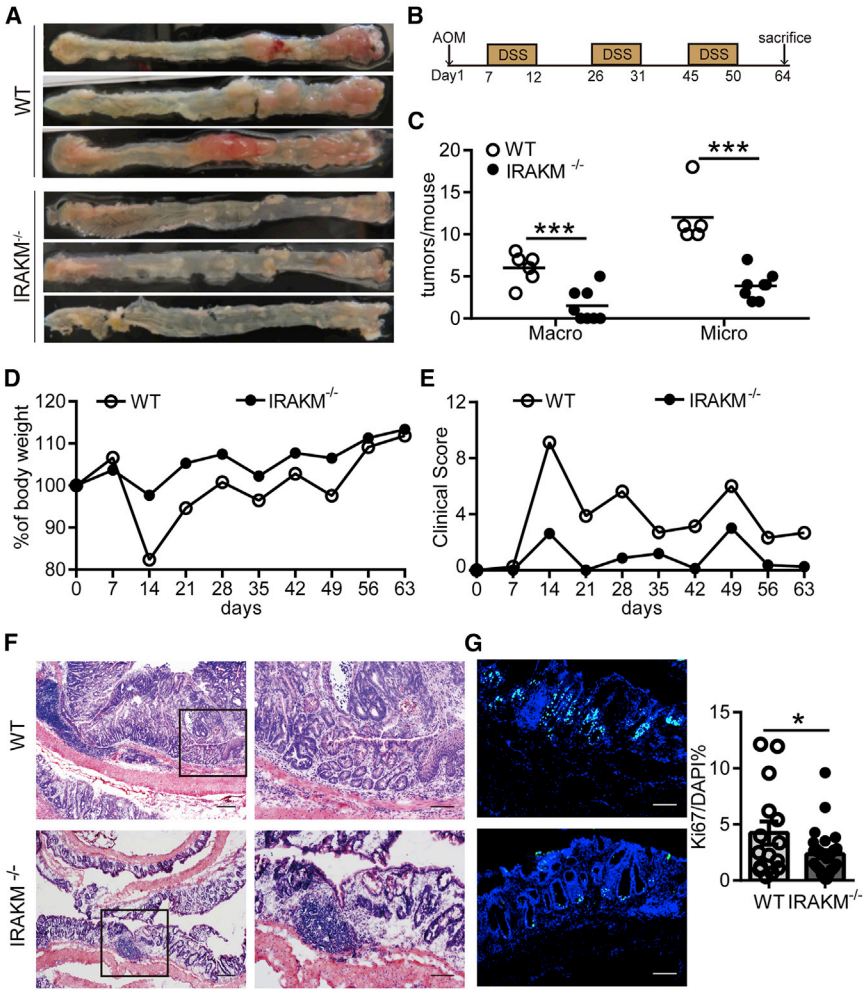

Figure 1. *IRAK-M*$^{-/-}$ Mice Are Protected against AOM/DSS-Driven Colon Tumorigenesis

(A) Representative images of colon tissues from WT and IRAK-M$^{-/-}$ mice treated with AOM/DSS. (B) A schematic protocol of AOM/DSS treatment. (C) Colon tumor counts in WT (n = 6) and IRAK-M$^{-/-}$ (n = 8) mice. Diameter of tumors greater than or equal to 2 mm defined as "macro" tumor; diameter of tumors less than 2 mm defined as "micro" tumor. (D) Body weight changes of WT (n = 6) and IRAK-M$^{-/-}$ (n = 8) mice throughout the AOM/DSS treatment. (E) Stool clinical scores including stool consistency and bleeding of WT (n = 6) and IRAK-M$^{-/-}$ (n = 8) mice. Values were expressed as means. (F) H&E-stained sections of colon from WT or IRAK-M$^{-/-}$ mice with AOM/DSS treatment. Scale bars represent 200 μm (left) and 100 μm (right), respectively. (G) Immunofluorescent analysis of Ki67 staining in colons from WT or IRAK-M$^{-/-}$ mice treated with AOM/DSS and quantitative analysis of Ki67 staining. Scale bars represent 100 μm. Data (C and G), mean ± SEM. Data (D and E), mean only. Student's t test (C and G). *p < 0.05; ***p < 0.001.

IRAK-M deficiency could potentially reprogram neutrophils from an immune-suppressive to an immune-enhancing phenotype. To further test this hypothesis, we next examined CD4 and CD8 T cell levels and their activities. As shown in Figure 3A, the percentages of splenic CD4 T cells were significantly and persistently higher in IRAK-M$^{-/-}$ mice than that in WT mice with or without AOM/DSS treatment. Meanwhile, the percentages of splenic CD8 T cells from IRAK-M$^{-/-}$ mice were similar to WT mice before AOM/DSS treatment but were higher than WT mice after AOM/DSS treatment (Figure 3B). In addition, we also observed that the percentages of colonic CD8 T cells from IRAK-M$^{-/-}$ mice were higher than those from WT mice after AOM/DSS treatment (Figure S1). Consistent with elevated T cell populations, Ki67 staining was much higher in T cells from IRAK-M$^{-/-}$ mice than from WT mice (Figure 3C). Furthermore, the expression of PD-1, an immune checkpoint, was significantly downregulated in T cells from IRAK-M$^{-/-}$ mice (Figure 3D). The percentage of Foxp3^{+} T cells was also lower in IRAK-M$^{-/-}$ mice than in WT mice (Figure 3E). Meanwhile, T cell activation in the spleen of IRAK-M$^{-/-}$ mice was enhanced, as reflected with a higher level of CD40L (Figure 3F) on CD4 T cells, as well as a higher level of CD107α on CD8 T cells (Figure 3G).

In addition to elevated T cell populations and activities, we also observed that the IRAK-M$^{-/-}$ mice expressed higher plasma levels of tumor necrosis factor alpha (TNF-α), interferon-γ (IFNγ), and interleukin-12 (IL-12), which are key cytokines involved in anti-tumor response induced by activation of Toll-like receptor (TLR)-family members following AOM/DSS challenge[26] (Figure S2). Intriguingly, we observed reduced circulating inflammatory cytokine IL-1β and increased anti-inflammatory mediator TGF-β in IRAK-M$^{-/-}$ mice challenged with AOM/DSS as compared to WT mice (Figure S2). Taken together, our data revealed that IRAK-M deficiency contributed to an enhanced anti-tumor T cell function, potentially through rewired neutrophils with enhanced immune-activating signals.

IRAK-M Mediates the Immunosuppressive Effects of Neutrophils on T Cell Proliferation and Activation via Reduced CD80/CD40 and Enhanced PD-L1

To further test the hypothesis that IRAK-M may facilitate the suppressive effects of neutrophils on T cells, we performed *in vitro* co-culture studies to test the effects of neutrophils on T cell proliferation and activation. We first purified and cultured bone marrow neutrophils from WT or IRAK-M$^{-/-}$ mice in complete medium with GM-CSF overnight. Consistent with our observation *in vivo* (Figure 2), we observed significantly elevated CD80 and CD40 expression and reduced PD-L1 level on IRAK-M$^{-/-}$ neutrophils cultured *in vitro*

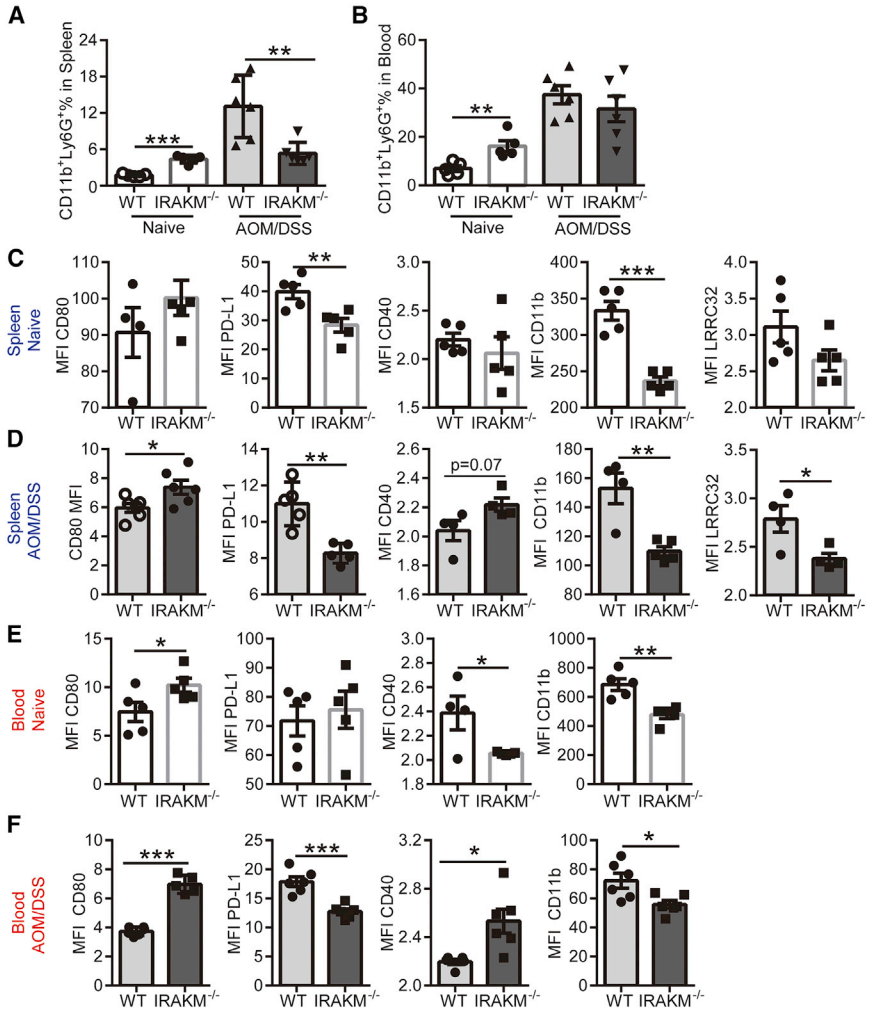

Figure 2. Enhanced CD80/CD40 Expression and Reduced Expression of PD-L1 and CD11b on IRAK-M$^{-/-}$ Neutrophils

(A and B) Percentages of neutrophils (Ly6G$^+$CD11b$^+$) in spleen (A) and blood (B) from naive mice or mice with AOM/DSS treatment. (C and D) CD80, PD-L1, CD40, CD11b, and LRRC32 expression on spleen neutrophils from naive mice (C) or mice with AOM/DSS treatment (D). (E and F) CD80, PD-L1, CD40, and CD11b expression on blood neutrophils from naive mice (E) or mice with AOM/DSS treatment (F). Data, mean ± SEM. Student's t test (C and G). *p < 0.05; **p < 0.01; ***p < 0.001.

(Figure 4A). We subsequently co-cultured the purified WT or IRAK-M$^{-/-}$ neutrophils together with 5,6-carboxyfluorescein diacetate succinimidyl (CFSE)-labeled allogeneic T cells in anti-CD3-coated plates. We observed that granulocyte-macrophage colony-stimulating factor (GM-CSF)-primed WT neutrophils exhibited a typical immunosuppressive phenotype, as reflected by reduced T cell proliferation co-cultured with WT neutrophils (Figure 4B). In contrast to the WT neutrophils, IRAK-M$^{-/-}$ neutrophils had significantly less immunosuppressive effects on the proliferation of CD4 and CD8 T cells, as shown with increased CFSE-negative CD4 and CD8 T cells (Figure 4B).

In addition to T cell proliferation, we further measured the effects of IRAK-M$^{-/-}$ neutrophils on key markers of T cell activation/suppression. As shown in Figure 4C, CD4 T cells co-cultured with IRAK-M$^{-/-}$ neutrophils exhibited a reduction of suppressive cell-surface marker PD-1 as well as nuclear levels of Foxp3 as compared to CD4 T cells co-cultured with WT neutrophils. In contrast, the populations of CD4 T cells expressing higher levels of co-stimulatory molecules, such as CD40L$^+$ and CD62L^{low}, were significantly increased when co-cultured with IRAK-M$^{-/-}$ neutrophils as compared to CD4 T cells co-cultured with WT neutrophils (Figure 4C). With regard to CD8 T cells, we observed that the expression levels of CD107α on CD8 T cells co-cultured with IRAK-M$^{-/-}$ neutrophils were significantly elevated, as well as the production of granzyme B and IFNγ (Figure 4D). On the other hand, PD-1 expression levels on CD8T cells co-cultured with IRAK-M$^{-/-}$ neutrophils were reduced as compared to CD8 T cells co-cultured with WT neutrophils (Figure 4D). These data further confirm that T cell activation was enhanced when co-cultured with IRAK-M$^{-/-}$ neutrophils as compared to WT neutrophils.

We next tested whether the elevated CD80/CD40 and reduced PD-L1 levels on IRAK-M neutrophils may collectively contribute to the enhancement of T cell activation. In the presence of anti-CD80 antibody during the co-culture, we observed that the proliferation of CD4 or CD8 T cells co-cultured with IRAK-M$^{-/-}$ neutrophils were blocked (Figure 5A). Furthermore, the addition of anti-CD80 reduced the activation markers of CD4 and CD8 T cells, reflected in reduced percentages of CD62L^{low}, CD40L$^+$, and CD107α$^+$ cells, respectively (Figures 5B and 5C). Similarly, in the presence of anti-CD40 antibody, T cell proliferation (Figure 5D), as well as T cell activation (Figures 5,E and 5F) co-cultured with IRAK-M$^{-/-}$ neutrophils, were also partially blocked. Consistent with previous reports, in the presence of anti-PD-L1 antibody, the suppression of WT neutrophils on T cell proliferation was partially released (Figure 5G). The application of anti-PD-L1 also lowered the levels of PD-1 on T cells and increased the population of CD62L^{low} CD4 T cells as well as the population of granzyme B-expressing CD8 T cells (Figures 5H and 5I). Collectively, our data suggest that increased CD80 and CD40 expression and decreased PD-L1 expression on IRAK-M$^{-/-}$ neutrophils are responsible for the reduced suppressive effects on T cell proliferation and activation.

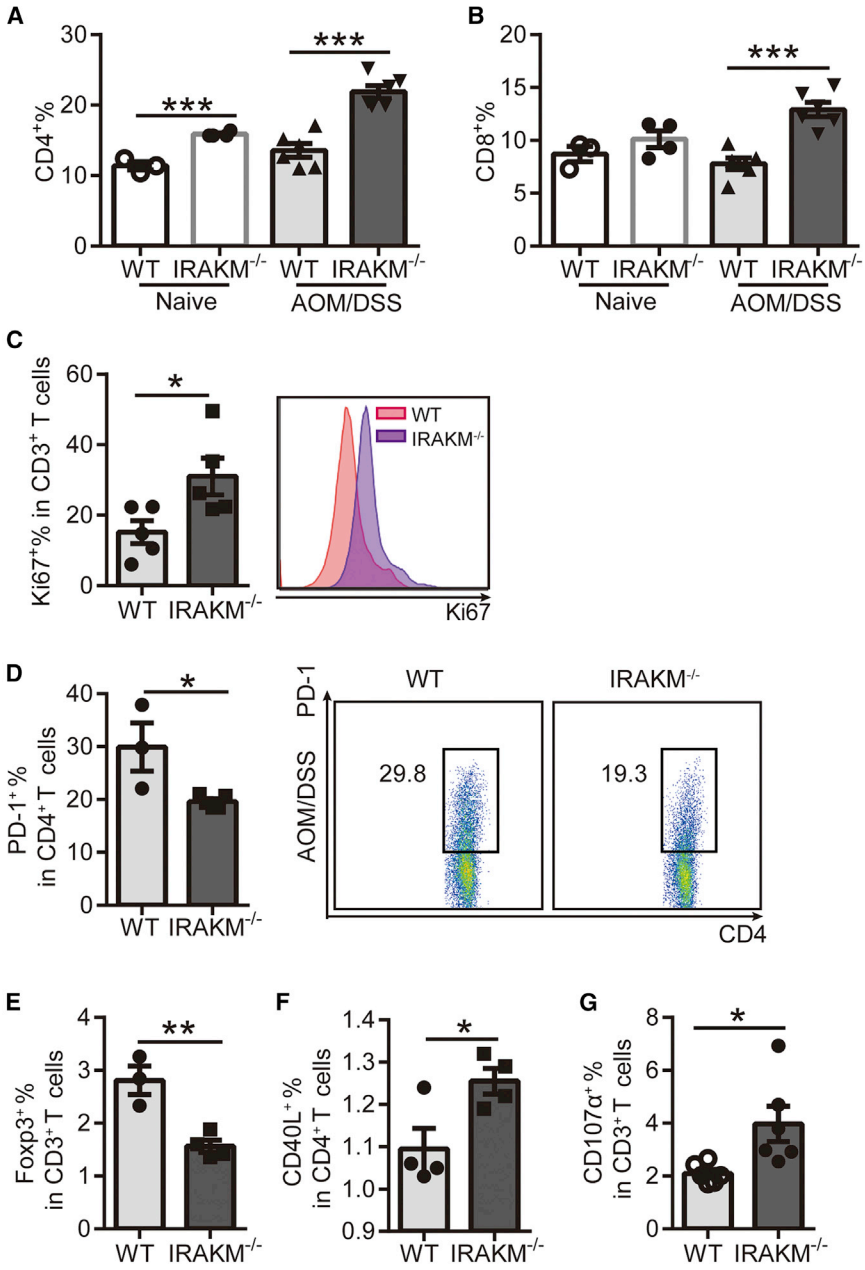

Figure 3. Enhanced T Cell Anti-tumor Responses in IRAK-M$^{-/-}$ Mice Challenged with AOM/DSS

(A and B) Percentages of CD4 T cell (A) and CD8 T cell (B) cells in the spleen from naive mice or mice with AOM/DSS treatment. (C–G) Activation status and proliferating ability of T cells in the spleen were tested in mice subjected to AOM/DSS treatments. (C) Ki67 expression on the CD3 T cells and representative flow histogram. (D) PD-1 expression on CD4 T cells and representative flow plots. (E) Foxp3 expression on the CD3 T cells. (F) CD40L expression on CD4 T cells. (G) CD107α expression on the CD3 T cells. Data, mean ± SEM. Student's t test. *$p < 0.05$; **$p < 0.01$; ***$p < 0.001$.

To clarify the underlying molecular mechanisms responsible for the neutrophil reprogramming due to IRAK-M deficiency, we analyzed pathways that are known to be critical in immune-regulation, such as STAT1/3/5 pathways. Previous studies reported that STAT1/3 and STAT5 are differentially involved in the expression of PD-L1 and CD80, with STAT1/3 promoting the expression of PD-L1[27–29] and STAT5 promoting the expression of CD80 and CD40.[30,31] We observed that the decreased phosphorylation level of STAT1/3 and increased phosphorylation level of STAT5 in IRAK-M$^{-/-}$ neutrophils as compared to WT neutrophils (Figure 5J), consistent with reduced PD-L1 expression and enhanced CD80 and CD40 expression in IRAK-M$^{-/-}$ neutrophils. STAT3 was shown to not only enhance tumor cell proliferation, but also inhibit the production of multiple pro-inflammatory cytokines and chemokines.[32] Thus, the elevated STAT5 activation and reduced STAT1/3 activation due to IRAK-M deficiency as shown above may be responsible for the rewiring of IRAK-M$^{-/-}$ neutrophils in restoring the responsiveness of tolerant anti-cancer immunity (Figure 5K).

Adoptive Transfer of IRAK-M$^{-/-}$ Neutrophils Is Sufficient to Dampen Colitis-Associated Tumor Progress

Given our findings that IRAK-M deficiency in neutrophils could potently release immunosuppression of neutrophils on T cells and enhance T cell anti-tumor response, we next tested whether these neutrophils could alleviate AOM/DSS-induced CRC. Purified neutrophils from either WT or IRAK-M$^{-/-}$ mice were transfused weekly to WT mice challenged with AOM/DSS as described in the Materials and Methods (Figure S3A). We chose the weekly injection regimen based on the previous reports that mature circulating neutrophils can survive ~6 days *in vivo* and that inflammatory conditions may further expand the lifespan of neutrophils.[33,34] During the course of AOM/DSS treatment, mice receiving IRAK-M$^{-/-}$ neutrophils displayed much lower disease scores (Figure S3B) and reduced body weight loss (Figure S3C), indicating an attenuation of disease progression compared to the mice receiving WT neutrophils. In addition, mice transferred with IRAK-M$^{-/-}$ neutrophils had a 2-fold reduction in both "micro" (5.0 ± 0.9) and "macro" (2.2 ± 0.7) polyps of colon, compared to that (9.8 ± 0.4; 4.25 ± 0.5) in mice transferred with WT neutrophils (Figures 6A and 6B). H&E staining revealed reduced inflammation and tumor load in mice transfused with IRAK-M$^{-/-}$ neutrophils (Figure 6C). Immunostaining displayed that the colons from mice transfused with IRAK-M$^{-/-}$ neutrophils had reduced Ki67-positive cells

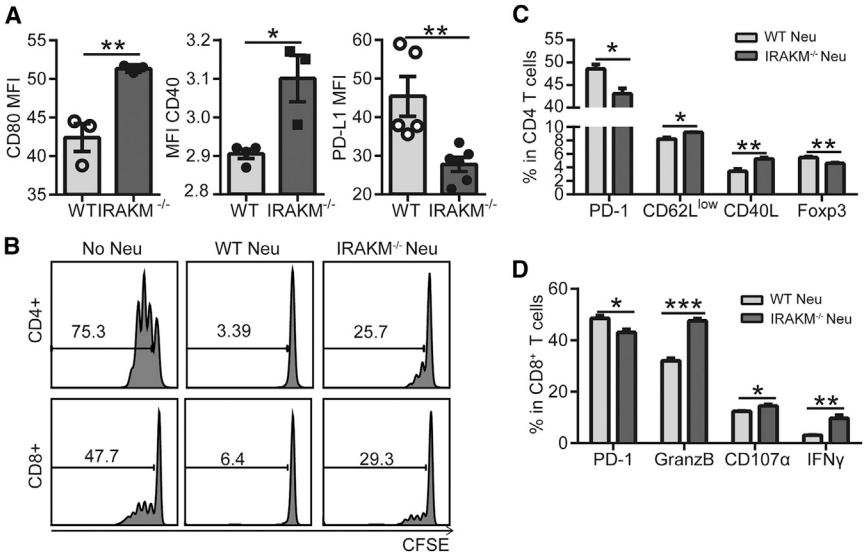

Figure 4. IRAK-M Deficiency Releases the Neutrophil Suppression on the Proliferation and Activation of T Cells

(A) CD80, CD40, and PD-L1 expression on GM-CSF primed WT or IRAK-M$^{-/-}$ neutrophils. (B) To monitor T cell proliferation, CFSE-labeled T cells were co-cultured with GM-CSF primed WT or IRAK-M$^{-/-}$ neutrophils in the anti-CD3 antibody-coated plates for 72 h. Representative results are shown. (C and D) To monitor T cell activation, PD-1, CD40L, CD62L, Foxp3, on CD4 T cells (C), as well as PD-1, granzyme B, IFNγ, and CD107α in CD8 T cells (D) were analyzed using flow cytometry. Data, mean ± SEM. Student's t test. *$p < 0.05$; **$p < 0.01$; ***$p < 0.001$.

(Figure 6D), suggesting a significant reduction in proliferating cell number, compared to mice transfused with WT neutrophils. Our data indicate that the transfusion of IRAK-M$^{-/-}$ neutrophils can be effectively used to render protection against AOM/DSS-induced colon tumorigenesis.

We further examined the cell counts and activation status of CD4 and CD8 T cells in mice challenged with AOM/DSS and transfused with WT or IRAK-M$^{-/-}$ neutrophils. As shown in Figure 6E, mice transfused with IRAK-M$^{-/-}$ neutrophils had more splenic cell counts of CD8 T cells. Furthermore, CD4 and CD8 T cells in mice transfused with IRAK-M$^{-/-}$ neutrophils demonstrated significantly elevated activation status, as reflected in the higher percentages of CD62L^{low} and CD40L^{+} in CD4 T cells (Figures 6H and 6J), as well as higher percentages of CD107a^{+} and CD62L^{low} in CD8 T cells (Figures 6F and 6J). In addition to activation, the proliferation of T cells in mice transfused with IRAK-M$^{-/-}$ neutrophils was also significantly elevated as shown by higher Ki67 expression in both CD4 and CD8 T cells (Figure 6I). Correlated with elevated T cell population and activation, mice transfused with IRAK-M$^{-/-}$ neutrophils had higher circulating levels of anti-tumor cytokines, such as TNF-α, IL-12, and lower levels of inflammatory cytokine IL-1β following AOM/DSS challenge (Figure 6K). Our data reveal that IRAK-M$^{-/-}$ neutrophils can effectively induce an enhanced anti-tumor immunity through facilitating T cell proliferation and activation *in vivo*.

DISCUSSION

Neutrophils are increasingly recognized to play critical roles in dampening anti-cancer immune responses through expressing co-inhibitory molecules such as PD-L1.[12,35] The molecular mechanisms for the generation of immune-suppressive neutrophils were not well understood. Our current study reveals that IRAK-M contributes to the generation of immune-suppressive neutrophils through rewiring cellular pathways involved in the differential expression of immune stimulatory and inhibitory molecules. We found that IRAK-M-deficient neutrophils have elevated expression of immune-enhancing molecules such as CD40 and CD80. In contrast, we observed that IRAK-M-deficient neutrophils have reduced expression of immune-inhibitory molecules such as PD-L1 and CD11b. We documented that IRAK-M-deficient neutrophils exhibit immune-enhancing functions, as reflected in the promotion of T cell proliferation and activation both *in vitro* and *in vivo*. At the translational level, IRAK-M-deficient neutrophils can boost anti-cancer immune defense in the murine model of inflammation-induced CRC.

Our findings complement and extend previous reports about the significant roles that neutrophils play during the course of cancer progression.[4,5,10,17] Human CRC patients were known to have elevated neutrophils with immune-suppressive properties.[36,37] Experimental animals with inflammation-induced CRC have also been documented with significant infiltration of immune-suppressive neutrophils, with key characteristics of elevated co-inhibitory molecules such as PD-L1 as well as other cell-surface markers such as CD11b.[12,38] In agreement with these reports, our data show that WT neutrophils indeed exhibit immune-suppressive functions with elevated levels of PD-L1 and CD11b. Furthermore, our *in vitro* functional assays confirm an immune-suppressive phenotype of wild-type neutrophils co-cultured with either CD4 or CD8 T cells. Despite the well-recognized phenotype, the underlying molecular mechanisms have not been well understood. Given the putative role of IRAK-M in suppressing innate macrophages, we tested whether IRAK-M may also be involved in the generation of immune-suppressive neutrophils. Our data confirm that IRAK-M-deficient neutrophils do not exhibit immune-suppressive function toward either CD4 or CD8 T cells. In contrast to WT immune-suppressive neutrophils, IRAK-M-deficient neutrophils have reduced expression of immune-suppressive PD-L1 and CD11b. In addition, out data show that IRAK-M-deficient neutrophils have elevated expression of CD40 and CD80, which are known co-stimulatory molecules promoting T cell proliferation and activation.[39,40] Together, our study reveals that the innate suppressor IRAK-M is at least partially responsible for the establishment of

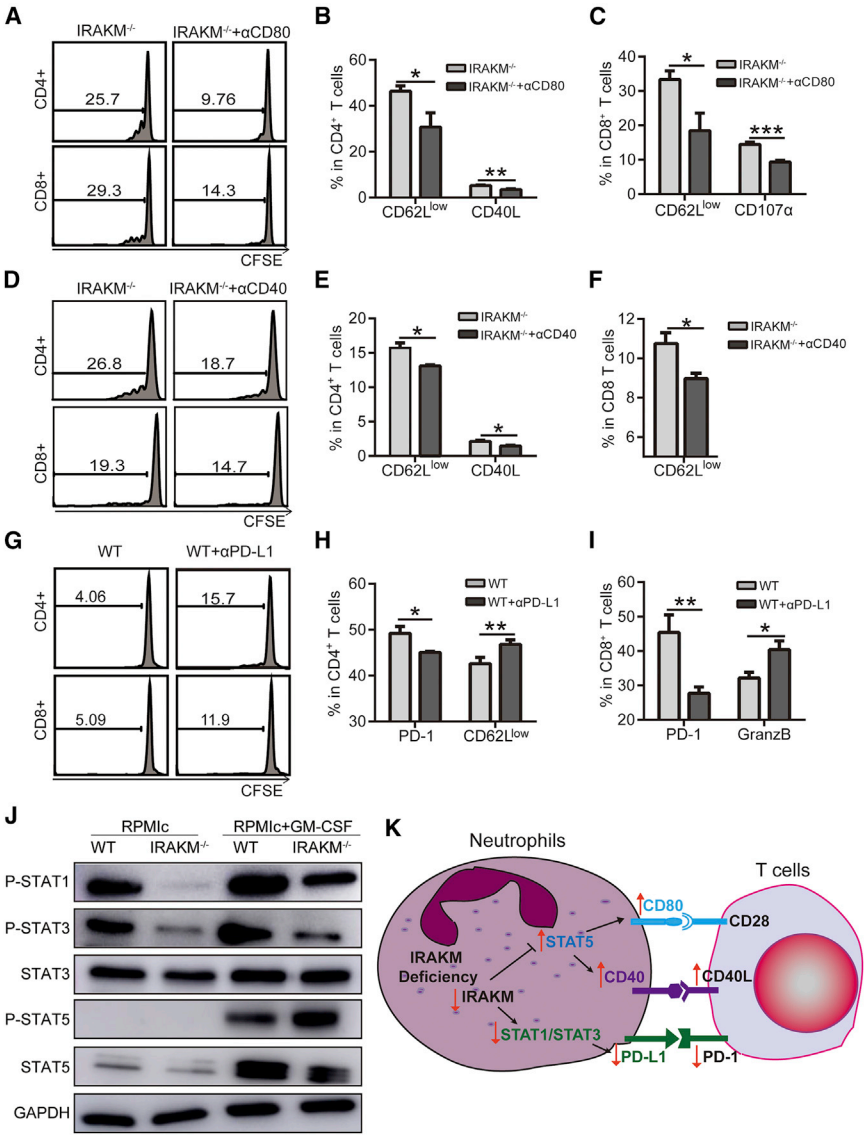

Figure 5. IRAK-M Deficiency Mediates the Neutrophil Suppression on the Proliferation and Activation T Cells via Enhanced CD80/CD40 and Reduced PD-L

To monitor T cell proliferation, CFSE-labeled T cells were co-cultured with GM-CSF primed neutrophils in the anti-CD3 antibody-coated plates for 72 h, without or with anti-CD80 antibody (A), anti-CD40 antibody (D), or anti-PD-L1 antibody (G). To monitor T cell activation, PD-1, CD40L, CD62L on CD4 T cells, as well as CD62L, PD-1, granzyme B, IFNγ, and CD107α in CD8 T cells were analyzed using flow cytometry. (B and C) In the presence of anti-CD80 antibody, CD62L, CD40L on CD4 T cells (B), and CD62L and CD107α on $CD8^+$ cells (C) were analyzed by flow cytometry. (E and F) In the presence of anti-CD40 antibody, CD62L, CD40L on CD4 T cells (E), and CD62L on CD8 T cells (F) were analyzed by flow cytometry. (H and I) In the presence of anti-PD-L1 antibody, CD62L, PD-1 on CD4 T cells (H), and PD-1 and granzyme B on CD8 T (I) cells were analyzed by flow cytometry. (J) Immunoblotting analysis of p-STAT1, p-STAT3, STAT3, p-STAT5, STAT5, and GAPDH in lysates from bone marrow neutrophils primed with or without GM-CSF overnight. (K) Schematic diagram of the role and regulation of IRAK-M in neutrophils with T cell communication. Data, mean ± SEM. Student's t test. *$p < 0.05$, **$p < 0.01$, ***$p < 0.001$.

immune-suppressive neutrophils and that the removal of IRAK-M can re-program neutrophils into an immune-enhancing state.

Our data are consistent with the previous report that IRAK-M levels are significantly upregulated in patients with inflammatory bowel disease (IBD), CRC, and colitis associated cancer (CAC).[23] Our data also complement another independent study showing that IRAK-M supports inflammation-driven CRC progression through the reduction of anti-microbial defenses and the stabilization of STAT3.[24] Our study confirms that IRAK-M is not only involved in the activation of STAT3 within neutrophils, but also responsible for the activation of STAT1. The inhibitory molecule PD-L1 expression was shown to be under the control of STAT1 and STAT3.[28,41] We show herein that IRAK-M deficiency in neutrophils leads to reduced activation of STAT1/3, corresponding to the reduced expression of PD-L1 on neutrophils. On the other hand, STAT5 is responsible for the expression of co-stimulatory molecules such as CD80 and CD40.[30,31] We document that IRAK-M-deficient neutrophils have elevated STAT5 levels and enhanced expression of CD80/CD40. Our correlational data suggest that IRAK-M may support the generation of immune-suppressive neutrophils and formation of immune-tolerant tumor microenvironment through differential regulation of STAT1/3 and STAT5 pathways. Our study is consistent with emerging studies that STAT1/3 and STAT5 may be mutually competitive and form complex feedback loops in regulating gene expressions.[42] However, other transcriptional modulators in addition to STATs may also be required to ensure an orderly expression of distinct effector molecules.[43] The complex integration of transcriptional networks involving multiple transcriptional modulators are likely responsible for the dynamic modulation of stimulatory versus inhibitory molecules on neutrophils. Extensive future mechanistic studies are needed to better define the detailed signaling networks responsible for the unique reprogramming of neutrophils due to IRAK-M deletion.

Collectively, our data reveal an important role of IRAK-M in the generation of immunosuppressive neutrophils. IRAK-M deletion reprograms neutrophils into an immune-enhanced state with the capability to promote, instead of suppress, the proliferation and activation of

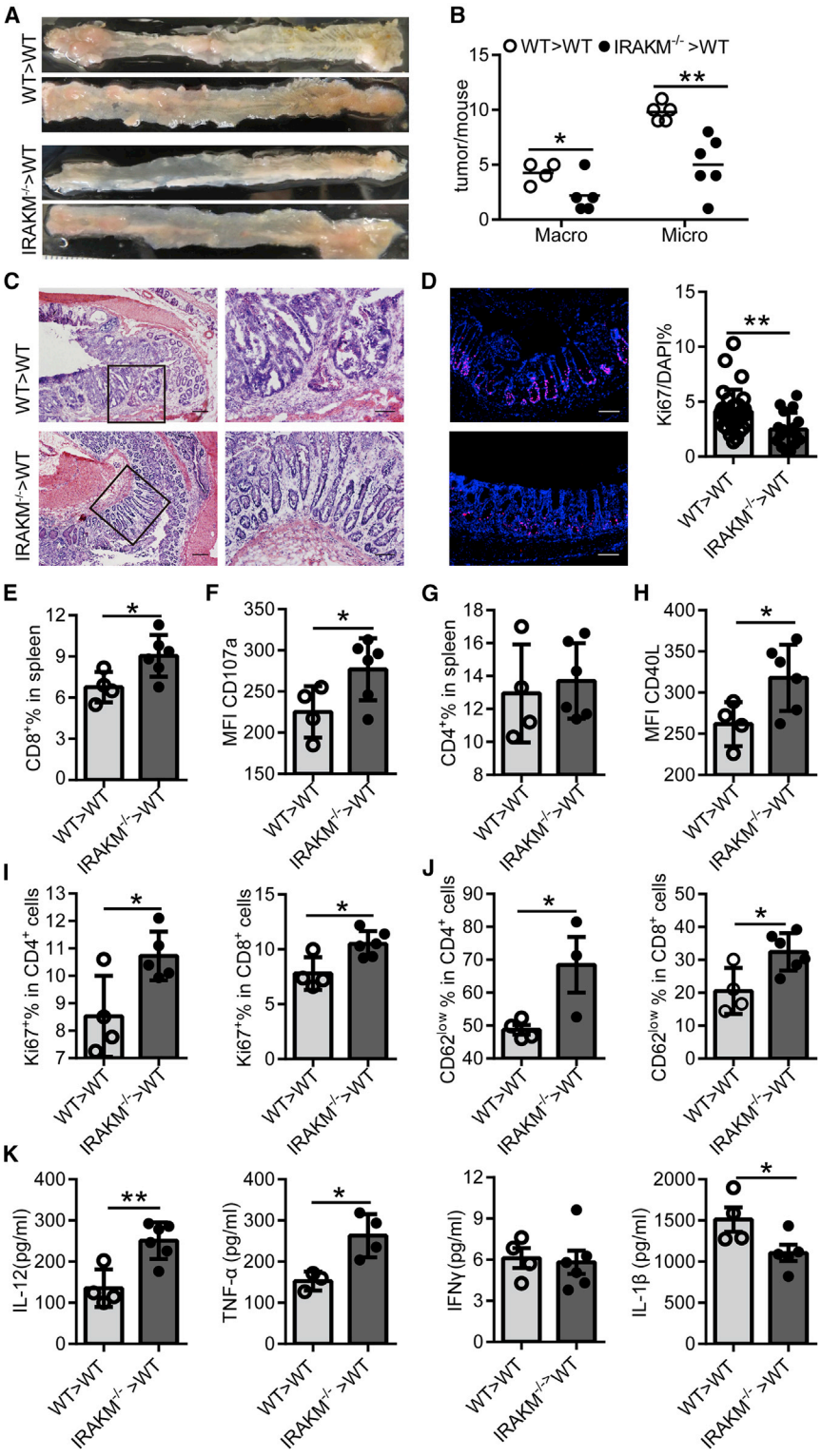

Figure 6. Transfusion of IRAK-M$^{-/-}$ Neutrophils to WT Mice Slows Down Colitis-Associated Colon Cancer Progression through Enhancing Anti-tumor Immune Response

(A) Representative images of colons from WT mice received WT or IRAK-M$^{-/-}$ neutrophils at the end of the experimental regimen. (B) Tumor counts in WT mice received WT (n = 5) or IRAK-M$^{-/-}$ (n = 6) neutrophils. (C) H&E-stained sections of colon tissues from mice received WT or IRAK-M$^{-/-}$ neutrophils. Colon tissues were collected in swiss rolls at the end of the AOM/DSS regimen. Scale bars represent 200 μm (left) and 100 μm (right), respectively. (D) Immunofluorescent analysis of Ki67 (red). Blue color represents DAPI staining. Scale bar represents 100 μm. Data (B and F), mean ± SEM. Data (C and D), mean only. Student's t test (C and G). *p < 0.05; **p < 0.01. (E and F) CD8 T cell counts (E) and CD107a expression on CD8 T cell (F) in the spleens from the mice that received WT or IRAK-M$^{-/-}$ neutrophils. (G and H) CD4 T cell counts (G) and CD40L expression (H) on CD4 T cell in the spleens from the mice that received WT or IRAK-M$^{-/-}$ neutrophils. (I and J) Representative flow images and graphical representation of Ki67 (I) and CD62L expression (J) on CD4 and CD8 T cells. (K) Cytokine profiles of plasma collected from mice that received WT or IRAK-M$^{-/-}$ neutrophils. Data, mean ± SEM. Student's t test. *p < 0.05, **p < 0.01, ***p < 0.001.

effective T cells both *in vitro* and *in vivo*. Our adoptive transfer data with IRAK-M-deficient neutrophils *in vivo* further support the translational potential of reprogrammed neutrophils in cancer treatment. Our study suggests that IRAK-M deletion, inhibition, or degradation could potentially be used to reprogram innate leukocytes such as neutrophils into an immune-enhanced phenotype, which may overcome immunosuppression and augment the host response to check point inhibition when used in combination therapy. Future studies of IRKA-M in human neutrophils and tumor environment are needed in order to better harness the therapeutic potential of targeting IRAK-M in neutrophils.

MATERIALS AND METHODS

Experimental Mice

All mouse studies were performed in accordance with the Federal NIH Guide for the Care and Use of Laboratory Animals and approved by the Institute for Animal Care and Use Committee (IACUC) at Virginia Tech. The *IRAK-M*$^{-/-}$ mice were generated as previously described[21] and purchased from The Jackson Laboratory. All studies were controlled with either littermate and/or co-housed WT animals that were maintained under specific pathogen-free conditions and received standard chow and water *ad libitum*.

Experimental Colitis-Associated Tumorigenesis

Tumorigenesis was induced in matched WT and IRAK-M$^{-/-}$ mice (8–10 weeks of age and 25–30 g weight) via a single intraperitoneal (i.p.) injection of AOM (10 mg/kg of total bodyweight, Sigma-Aldrich) and supplemented with three cycles of 2% DSS in drinking water available *ad libitum* for 5 days with 2 weeks of recovery between cycles. While subjected to DSS, mice were monitored for weight loss, physical body condition, stool consistency, and rectal bleeding. After the last water cycle, mice were sacrificed and tissues were harvested for further analysis. A schematic protocol was illustrated in Figure 1B. Polyp formation was classified as "macro" and "micro" polyp depending on the size equal to or greater than 2 mm versus less than 2 mm, respectively.

Adoptive Transfer of Neutrophils

Bone marrow cells were isolated from WT or IRAK-M$^{-/-}$ mice and were purified using EasySep Mouse Neutrophil Enrichment Kit (Stem Cell) with >95% purity, according to the manufacturer's instruction. Recipient WT mice were transfused with 3.5–5 $\times$ 10^6 neutrophils in 200 μL PBS twice (post-DSS day 5 and day 12) per DSS-resting cycle through intravenous injection. Detailed timeline was illustrated in Figure S3. One day after the last cell transfer, mice were sacrificed and tissues were harvested for subsequent analyses.

Histological Analyses

Histological analyses were performed on fresh-frozen and optimal cutting temperature (OCT) embedded colon tissue sections. Slides were fixed in 4% neutral buffered formalin for 5 min, followed by H&E staining. For immunofluorescence staining, sections were fixed in 4% neutral buffered formalin for 5 min and stained with anti-mouse primary antibodies (Ki67, Abcam, 1:100) followed by a biotinylated anti-immunoglobulin (Ig) secondary Ab (BD eBiosciences) and streptavidin-fluorescein isothiocyanate (FITC). DAPI was used to stain nucleus. Six viewing fields from each slide were captured under fluorescent microscope. Pixel values reflecting the fluorescent intensities of each viewing field were quantitated with the NIH ImageJ software.

Flow Cytometry

To analyze neutrophil phenotype, cells were stained with anti-Ly6G, anti-CD11b, anti-PD-L1, anti-CD80, anti-CD40, and anti-LRRC32 from BioLegend. To analysis T cell phenotype, antibodies such as anti-CD3, anti-CD4, anti-CD8, anti-CD40L, anti-CD62L, anti-PD-1, anti-IFNγ, anti-Foxp3, anti-GranzymB, and anti-Ki67 from BioLegend were used. Stained cells were analyzed with a FACS-Canto II (BD Biosciences). The data were processed by Flow Jo (Ashland, OR).

T Cell Proliferation Assay

Splenocytes were purified using EasySep Mouse T Cell Isolation Kit (Stem Cell), according to the manufacturer's instruction, then were labeled with CFSE (Invitrogen, Molecular Probes), according to the manufacturer's instructions. CFSE-labeled T cells were stimulated with plate-bound anti-mouse CD3 (5 μg/mL) antibody (Bio X Cell; clone 145-2C11). Neutrophils purified from bone marrow were cultured in RPMI 1640 medium supplemented with 10% fetal bovine serum, 2 mM L-glutamine, 10 mM HEPES, 1% penicillin/streptomycin, and with GM-CSF (1 ng/mL) for 24 h. CFSE-labeled T cells were mixed with cultured neutrophils at a 1:1 ratio and co-cultured in CD3-coated plates for 72 h. CFSE signals were analyzed by flow cytometry on gated CD4 T cells and CD8 T cells. In blocking experiments, antibodies against CD80, PD-L1, and CD40 (BioLegend) were added to the co-culture at the concentration of 1 μg/mL.

Immunoblotting

Bone marrow neutrophils were purified by 65% percoll gradient, and the purity was >90% confirmed by flow cytometry with Ly6G^{+} CD11b^{+} staining. Purified BM neutrophils were cultured in complete RPMI medium with or without GM-CSF (1 ng/mL) overnight, and total cell lysate was extracted. Protein samples of equal amount were separated with SDS-PAGE and transferred to polyvinylidene fluoride (PVDF) membranes, which were probed anti-phospho STAT1, anti-phospho STAT3, anti-STAT3, anti-phospho STAT5, anti-STAT5, anti-phospho STAT3, anti-STAT3 and GAPDH antibody bought from Cell Signaling, and anti-rabbit or mouse IgG secondary antibody (Cell Signaling) according to the manufacturer's instructions. The immunoblots were developed by a chemiluminescence ECL detection kit (Thermo Fisher).

ELISA

For *in vivo* analyses, plasma was collected from the mice at time of sacrificing. The levels of TNF-α, IL-1β, IL-12, IFNγ, and TGF-β in plasma were measured using ELISA kits purchased from R&D Systems, according to the manufacturer's instructions.

Statistical Analysis

All experiments were performed at least three times. Representative and reproducible results were shown. Statistical analysis was performed with Prism software (GraphPad Software 6.0, La Jolla, CA). Data were expressed as means ± SEM. The significance of the differences was assessed by Student's t test (for two groups) or one-way ANOVA (for multiple groups). $p < 0.05$ was considered statistically significant.

SUPPLEMENTAL INFORMATION

Supplemental Information can be found online at https://doi.org/10.1016/j.ymthe.2019.09.019.

AUTHOR CONTRIBUTIONS

L.L., Y.Z., and N.D. designed the experiments. Y.Z., N.D., and L.L. developed the methodology. N.D., Y.Z., and C.K.L. conducted the experiments and collected the data. N.D., Y.Z., and L.L. analyzed and interpreted the data. L.L., N.D., Y.Z., L.B., and H.W.C. wrote, reviewed, and/or revised the manuscript. L.L. supervised the experiments.

CONFLICTS OF INTEREST

The authors declare no competing interests.

ACKNOWLEDGMENTS

We appreciate the technical assistance, discussion, and proofreading from the Li lab members at Virginia Tech.

REFERENCES

1. Edwards, B.K., Noone, A.M., Mariotto, A.B., Simard, E.P., Boscoe, F.P., Henley, S.J., Jemal, A., Cho, H., Anderson, R.N., Kohler, B.A., et al. (2014). Annual Report to the Nation on the status of cancer, 1975-2010, featuring prevalence of comorbidity and impact on survival among persons with lung, colorectal, breast, or prostate cancer. Cancer *120*, 1290–1314.

2. Markman, J.L., and Shiao, S.L. (2015). Impact of the immune system and immunotherapy in colorectal cancer. J. Gastrointest. Oncol. *6*, 208–223.

3. Amin, M., and Lockhart, A.C. (2015). The potential role of immunotherapy to treat colorectal cancer. Expert Opin. Investig. Drugs *24*, 329–344.

4. Powell, D.R., and Huttenlocher, A. (2016). Neutrophils in the Tumor Microenvironment. Trends Immunol. *37*, 41–52.

5. Shen, M., Hu, P., Donskov, F., Wang, G., Liu, Q., and Du, J. (2014). Tumor-associated neutrophils as a new prognostic factor in cancer: a systematic review and meta-analysis. PLoS ONE *9*, e98259.

6. Gentles, A.J., Newman, A.M., Liu, C.L., Bratman, S.V., Feng, W., Kim, D., Nair, V.S., Xu, Y., Khuong, A., Hoang, C.D., et al. (2015). The prognostic landscape of genes and infiltrating immune cells across human cancers. Nat. Med. *21*, 938–945.

7. Shaul, M.E., and Fridlender, Z.G. (2017). Neutrophils as active regulators of the immune system in the tumor microenvironment. J. Leukoc. Biol. *102*, 343–349.

8. Shaul, M.E., Levy, L., Sun, J., Mishalian, I., Singhal, S., Kapoor, V., Horng, W., Fridlender, G., Albelda, S.M., and Fridlender, Z.G. (2016). Tumor-associated neutrophils display a distinct N1 profile following TGFβ modulation: A transcriptomics analysis of pro- vs. antitumor TANs. OncoImmunology *5*, e1232221.

9. Sionov, R.V., Fridlender, Z.G., and Granot, Z. (2015). The Multifaceted Roles Neutrophils Play in the Tumor Microenvironment. Cancer Microenviron. *8*, 125–158.

10. Fridlender, Z.G., Sun, J., Kim, S., Kapoor, V., Cheng, G., Ling, L., Worthen, G.S., and Albelda, S.M. (2009). Polarization of tumor-associated neutrophil phenotype by TGF-beta: "N1" versus "N2" TAN. Cancer Cell *16*, 183–194.

11. Smyth, M.J., Ngiow, S.F., Ribas, A., and Teng, M.W. (2016). Combination cancer immunotherapies tailored to the tumour microenvironment. Nat. Rev. Clin. Oncol. *13*, 143–158.

12. Wang, T.T., Zhao, Y.L., Peng, L.S., Chen, N., Chen, W., Lv, Y.P., Mao, F.Y., Zhang, J.Y., Cheng, P., Teng, Y.S., et al. (2017). Tumour-activated neutrophils in gastric cancer foster immune suppression and disease progression through GM-CSF-PD-L1 pathway. Gut *66*, 1900–1911.

13. Sagiv, J.Y., Michaeli, J., Assi, S., Mishalian, I., Kisos, H., Levy, L., Damti, P., Lumbroso, D., Polyansky, L., Sionov, R.V., et al. (2015). Phenotypic diversity and plasticity in circulating neutrophil subpopulations in cancer. Cell Rep. *10*, 562–573.

14. Shaul, M.E., and Fridlender, Z.G. (2019). Tumour-associated neutrophils in patients with cancer. Nat. Rev. Clin. Oncol. *16*, 601–620.

15. García-Mendoza, M.G., Inman, D.R., Ponik, S.M., Jeffery, J.J., Sheerar, D.S., Van Doorn, R.R., and Keely, P.J. (2016). Neutrophils drive accelerated tumor progression in the collagen-dense mammary tumor microenvironment. Breast Cancer Res. *18*, 49.

16. Faget, J., Groeneveld, S., Boivin, G., Sankar, M., Zangger, N., Garcia, M., Guex, N., Zlobec, I., Steiner, L., Piersigilli, A., et al. (2017). Neutrophils and Snail Orchestrate the Establishment of a Pro-tumor Microenvironment in Lung Cancer. Cell Rep. *21*, 3190–3204.

17. Zhang, Y., Lee, C., Geng, S., and Li, L. (2019). Enhanced tumor immune surveillance through neutrophil reprogramming due to Tollip deficiency. JCI Insight *4*, 122939.

18. Xue, J., Zhao, Z., Zhang, L., Xue, L., Shen, S., Wen, Y., Wei, Z., Wang, L., Kong, L., Sun, H., et al. (2017). Neutrophil-mediated anticancer drug delivery for suppression of postoperative malignant glioma recurrence. Nat. Nanotechnol. *12*, 692–700.

19. Xue, Y., Wu, Y., Wang, Q., Xue, L., Su, Z., and Zhang, C. (2019). Cellular Vehicles Based on Neutrophils Enable Targeting of Atherosclerosis. Mol. Pharm. *16*, 3109–3120.

20. D'Aloia, M.M., Zizzari, I.G., Sacchetti, B., Pierelli, L., and Alimandi, M. (2018). CAR-T cells: the long and winding road to solid tumors. Cell Death Dis. *9*, 282.

21. Kobayashi, K., Hernandez, L.D., Galán, J.E., Janeway, C.A., Jr., Medzhitov, R., and Flavell, R.A. (2002). IRAK-M is a negative regulator of Toll-like receptor signaling. Cell *110*, 191–202.

22. Wesche, H., Gao, X., Li, X., Kirschning, C.J., Stark, G.R., and Cao, Z. (1999). IRAK-M is a novel member of the Pelle/interleukin-1 receptor-associated kinase (IRAK) family. J. Biol. Chem. *274*, 19403–19410.

23. Rothschild, D.E., Zhang, Y., Diao, N., Lee, C.K., Chen, K., Caswell, C.C., Slade, D.J., Helm, R.F., LeRoith, T., Li, L., and Allen, I.C. (2017). Enhanced Mucosal Defense and Reduced Tumor Burden in Mice with the Compromised Negative Regulator IRAK-M. EBioMedicine *15*, 36–47.

24. Kesselring, R., Glaesner, J., Hiergeist, A., Naschberger, E., Neumann, H., Brunner, S.M., Wege, A.K., Seebauer, C., Köhl, G., Merkl, S., et al. (2016). IRAK-M Expression in Tumor Cells Supports Colorectal Cancer Progression through Reduction of Antimicrobial Defense and Stabilization of STAT3. Cancer Cell *29*, 684–696.

25. Leliefeld, P.H.C., Koenderman, L., and Pillay, J. (2015). How neutrophils shape adaptive immune responses. Front. Immunol. *6*, 471.

26. Geng, D., Zheng, L., Srivastava, R., Velasco-Gonzalez, C., Riker, A., Markovic, S.N., and Davila, E. (2010). Amplifying TLR-MyD88 signals within tumor-specific T cells enhances antitumor activity to suboptimal levels of weakly immunogenic tumor antigens. Cancer Res. *70*, 7442–7454.

27. Marzec, M., Zhang, Q., Goradia, A., Raghunath, P.N., Liu, X., Paessler, M., Wang, H.Y., Wysocka, M., Cheng, M., Ruggeri, B.A., and Wasik, M.A. (2008). Oncogenic kinase NPM/ALK induces through STAT3 expression of immunosuppressive protein CD274 (PD-L1, B7-H1). Proc. Natl. Acad. Sci. USA *105*, 20852–20857.

28. Garcia-Diaz, A., Shin, D.S., Moreno, B.H., Saco, J., Escuin-Ordinas, H., Rodriguez, G.A., Zaretsky, J.M., Sun, L., Hugo, W., Wang, X., et al. (2017). Interferon Receptor Signaling Pathways Regulating PD-L1 and PD-L2 Expression. Cell Rep. *19*, 1189–1201.

29. O'Reilly, L.A., Putoczki, T.L., Mielke, L.A., Low, J.T., Lin, A., Preaudet, A., Herold, M.J., Yaprianto, K., Tai, L., Kueh, A., et al. (2018). Loss of NF-kappaB1 Causes Gastric Cancer with Aberrant Inflammation and Expression of Immune Checkpoint Regulators in a STAT-1-Dependent Manner. Immunity *48*, 570–583.e8.

30. Tormo, A.J., and Gauchat, J.F. (2013). A novel role for STAT5 in DC: Controlling the Th2-response. JAK-STAT *2*, e25352.

31. Natarajan, C., Sriram, S., Muthian, G., and Bright, J.J. (2004). Signaling through JAK2-STAT5 pathway is essential for IL-3-induced activation of microglia. Glia *45*, 188–196.

32. Wang, T., Niu, G., Kortylewski, M., Burdelya, L., Shain, K., Zhang, S., Bhattacharya, R., Gabrilovich, D., Heller, R., Coppola, D., et al. (2004). Regulation of the innate and adaptive immune responses by Stat-3 signaling in tumor cells. Nat. Med. *10*, 48–54.

33. Hidalgo, A., Chilvers, E.R., Summers, C., and Koenderman, L. (2019). The Neutrophil Life Cycle. Trends Immunol. *40*, 584–597.

34. Silvestre-Roig, C., Hidalgo, A., and Soehnlein, O. (2016). Neutrophil heterogeneity: implications for homeostasis and pathogenesis. Blood *127*, 2173–2181.

35. He, G., Zhang, H., Zhou, J., Wang, B., Chen, Y., Kong, Y., Xie, X., Wang, X., Fei, R., Wei, L., et al. (2015). Peritumoural neutrophils negatively regulate adaptive immunity via the PD-L1/PD-1 signalling pathway in hepatocellular carcinoma. J. Exp. Clin. Cancer Res. *34*, 141.

36. Ho, A.S., Chen, C.H., Cheng, C.C., Wang, C.C., Lin, H.C., Luo, T.Y., Lien, G.S., and Chang, J. (2014). Neutrophil elastase as a diagnostic marker and therapeutic target in colorectal cancers. Oncotarget *5*, 473–480.

37. Kim, J.H., Lee, J.Y., Kim, H.K., Lee, J.W., Jung, S.G., Jung, K., Kim, S.E., Moon, W., Park, M.I., and Park, S.J. (2017). Prognostic significance of the neutrophil-to-lymphocyte ratio and platelet-to-lymphocyte ratio in patients with stage III and IV colorectal cancer. World J. Gastroenterol. *23*, 505–515.

38. Pillay, J., Kamp, V.M., van Hoffen, E., Visser, T., Tak, T., Lammers, J.W., Ulfman, L.H., Leenen, L.P., Pickkers, P., and Koenderman, L. (2012). A subset of neutrophils in human systemic inflammation inhibits T cell responses through Mac-1. J. Clin. Invest. *122*, 327–336.

39. Sun, Y., Peng, D., Lecanda, J., Schmitz, V., Barajas, M., Qian, C., and Prieto, J. (2000). In vivo gene transfer of CD40 ligand into colon cancer cells induces local production of cytokines and chemokines, tumor eradication and protective antitumor immunity. Gene Ther. *7*, 1467–1476.

40. Radsak, M., Iking-Konert, C., Stegmaier, S., Andrassy, K., and Hänsch, G.M. (2000). Polymorphonuclear neutrophils as accessory cells for T-cell activation: major histocompatibility complex class II restricted antigen-dependent induction of T-cell proliferation. Immunology *101*, 521–530.

41. Sasidharan Nair, V., Toor, S.M., Ali, B.R., and Elkord, E. (2018). Dual inhibition of STAT1 and STAT3 activation downregulates expression of PD-L1 in human breast cancer cells. Expert Opin. Ther. Targets *22*, 547–557.

42. Wingelhofer, B., Neubauer, H.A., Valent, P., Han, X., Constantinescu, S.N., Gunning, P.T., Müller, M., and Moriggl, R. (2018). Implications of STAT3 and STAT5 signaling on gene regulation and chromatin remodeling in hematopoietic cancer. Leukemia *32*, 1713–1726.

43. Naranbhai, V., Fairfax, B.P., Makino, S., Humburg, P., Wong, D., Ng, E., Hill, A.V., and Knight, J.C. (2015). Genomic modulators of gene expression in human neutrophils. Nat. Commun. *6*, 7545.